

Shear strength of cast-in connectors in ultra-thin, ultra-high-performance-concrete panels with polyoxymethylene fibers

Hoda Osman and Amir Fam

- This paper examines the behavior of connectors in ultra-high-performance-concrete (UHPC) panels under direct shear loading. Different connector types were examined, including two threaded bolts (a carriage bolt and an L-shaped bolt) and two female headed inserts (a zamac insert and a flower-shaped insert).
- A total of 104 panels were fabricated and tested under shear loading with varying parameters for panel thickness, connector diameter, polyoxymethylene fiber content, support span length, and edge distance of the connector.
- A design equation is proposed for cast-in connectors in ultra-thin UHPC panels with polyoxymethylene fibers.

The focus of structural engineering research has recently shifted toward achieving more-sustainable and more-durable structures. The integration of double-wythe precast concrete insulated wall panels plays a crucial role in contributing to the sustainability of a building. This is achieved by improving energy efficiency and thus reducing the required energy expenditure. The incorporation of ultra-high-performance fiber-reinforced concrete (UHPFRC) into these structural elements produces wall panels that are significantly thinner than conventional sandwich panels. This, in turn, leads to panels that require less material, are more durable, and can speed up the construction process. This is a result of the mechanical properties of UHPFRC, mostly characterized by its compressive strength, which can range from 120 to 200 MPa (17.4 to 29 ksi). In addition, the incorporation of high-strength fibers into the mixture design also results in a prolonged postcracking tensile capacity reaching up to 15 MPa (2.2 ksi).¹⁻⁶ Because of the material's high strength and durability, thin precast ultra-high-performance concrete (UHPC) panels can also be used for a wide range of applications, including decking, flooring, and roofing.

Past researchers have investigated the behavior of UHPFRC in double-wythe precast concrete wall panels, also known as sandwich panels.^{7,8} These panels are typically used as exterior or interior walls and consist of two concrete wythes with an insulation layer, such as extruded polystyrene (XPS) or expanded polystyrene (EPS), in between the two wythes and can vary in thickness and type depending on the intended thermal resistance of the precast concrete wall.^{9,10} The two

concrete panels are connected using shear connectors, which enable the composite action designed for the panel.¹¹ Sylaj et al.⁷ and Sylaj and Fam⁸ investigated the incorporation of UHPFRC in sandwich panels by testing 25 mm (1 in.) thick concrete wythes under flexural, axial, and combined loading scenarios and concluded that the panels satisfied the deflection limitations required.

These precast concrete insulated wall panels are mechanically anchored to the frame of the building using varying connection types and installation methods. These include the use of cast-in or postinstalled connectors. These connections are used to resist axial and shear loads and securely fasten the panels to the frame of the structure. One of the loading scenarios includes the self-weight of the double-wythe precast concrete wall panels, which generates a shear force onto the embedded connectors.

The American Concrete Institute's *Building Code Requirements for Structural Concrete (ACI 318-19)* and *Commentary (ACI 318R-19)*¹² and the Canadian Standards Association's *Design of Concrete Structures (CSA A23.3:19)*¹³ codes state that connectors embedded in conventional concrete can have one of the following failure modes under shear loading (**Fig. 1**):

- steel failure (that is, the connector itself)
- concrete pryout
- concrete breakout

ACI 318-19 concrete breakout design was established using the concrete capacity design (CCD) method, which confirmed that the angle created from a breakout failure was at 35 degrees from the breakout failure surface.¹⁴ ACI 318-19 states that the estimated concrete breakout shear capacity V_u of a connector embedded in concrete should not exceed the smaller of Eq. (1) and (2), which adopted a 5% fractile to account for cracking. In addition, a modification factor was designed to be implemented in cases where the thickness of the panel was smaller than 1.5 times the edge distance of the connector.

$$V_u = 0.6 \left(\frac{l}{d_o} \right)^{0.2} \sqrt{d_o} \sqrt{f'_c} c^{1.5} \quad (1)$$

where

l = embedment (bearing) length

d_o = outer diameter of connector

f'_c = concrete compressive strength

c = edge distance to the free edge

$$V_u = 3.7 \sqrt{f'_c} c^{1.5} \quad (2)$$

Grosser et al.¹⁵ analyzed the behavior of single adhesive connectors installed in thick normal concrete slabs under shear loading near a free edge. The study varied the effect of different parameters on the breakout strength, including the diameter of the connector, embedment depth in the concrete, and edge distance. The shear capacities of the connectors were evaluated while varying the direction that the shear force was acting upon, including a shear force acting perpendicular, parallel, and oblique to the free edge of the panel. Following the experimental and numerical analyses, the study recommended slight modifications for the concrete breakout strength specifications for connectors subjected to shear loading (Eq. [3]).

$$V_u = 0.12 (d_o + 25) \left(\frac{l}{d_o} \right)^{0.2} \sqrt{f'_c} c^{\left(\frac{4}{3} \right)} \quad (3)$$

Tarawneh, Ross, and Cousins¹⁶ and Prejs, Jawdhari, and Fam¹⁷ studied the performance of postinstalled connectors in thin concrete members. Tarawneh, Ross, and Cousins¹⁶ analyzed the performance of adhesive and screw connectors fully embedded in concrete panel members ranging in thickness from 51 to 102 mm (2 to 4 in.). Other parameters varied in this study included connector diameter, edge distance, and the compressive strength of the concrete. After examining the behavior of 149 samples, the researchers addressed the predictability of the CCD method and the ACI 318-19 design equations. It was determined that the design equations underestimate the shear capacity as the embedment depth to edge distance ratio decreases below 1.5 and the design equations were modified accordingly to be used in thin panels. Similarly, Prejs, Jawdhari, and Fam¹⁷ studied postinstalled screw connectors and threaded rod connectors in thin UHPFRC panels. They compared the experimental results with the estimated shear capacity using the ACI standard, as well as the modified design equations to see if they would accurately predict the shear capacity. It was established that all the design equations overestimated the actual shear strength of postinstalled connectors in thin UHPFRC panels. As such, new design Eq. (4)

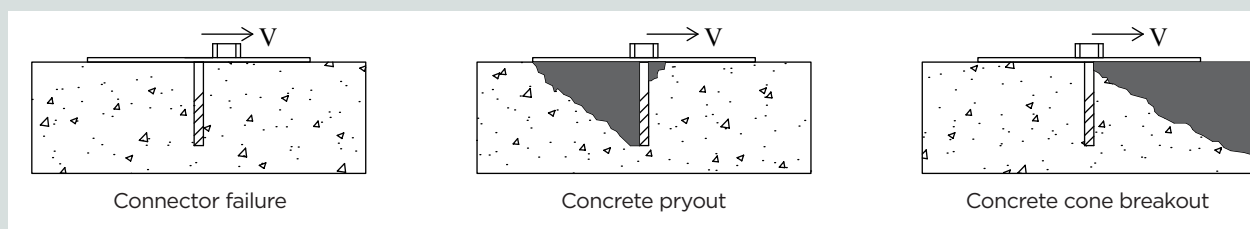


Figure 1. Different failure modes. Note: V = shear loading.

and (5) were developed:

The equation for screw connectors is as follows:

$$V_u = 5.73 \times 10^{-5} l^{0.65} d_o^{0.33} \sqrt{f'_c} c^{1.34} \quad (4)$$

The equation for threaded rod connectors is as follows:

$$V_u = 1.35 \times 10^{-3} l^{0.71} d_o^{0.03} \rho^{0.36} \sqrt{f'_c} c^{0.8} \quad (5)$$

where

ρ_f = fiber content by volume

Choi, Joh, and Chun¹⁸ investigated the behavior of cast-in connectors that were embedded in 100 mm (4 in.) thick UHPFRC panels and assessed the performance of these connectors under tensile and shear loads. The parameters studied involved variation in the embedment depth and the edge distance. Results showed a positive relationship between the embedment depth of the connectors and tensile and shear capacities. Compared with the predicted loads by the CCD method used for normal-strength concrete, the experimental loads of the cast-in connectors in UHPFRC panels enhanced the pullout capacities by a factor of 1.55 for connectors located in the center of the panel and by 1.23 for connectors located near the free edge of the panel. Choi, Joh, and Chun¹⁸ also deduced that the embedment of connectors in UHPFRC would result in enhanced shear capacities by a factor of 1.07. Consequently, a modified design Eq. (6) was developed for connections in UHPFRC panels that correspond to the breakout of those connections under shear loads.

$$V_u = 4.37 \left(\frac{l}{d_o} \right)^{\frac{1}{3}} \sqrt{d_o} \sqrt{f'_c} c \quad (6)$$

Although there have been thorough studies on the behavior of postinstalled connections in thin UHPFRC panels under shear loads, there is no known research that has investigated the shear capacity of cast-in (that is, preinstalled) connectors

in ultra-thin UHPFRC panels. This paper addresses this gap through the application of different cast-in connector types in ultra-thin UHPFRC panels tested under shear loading to investigate their feasibility and behavior.

Experimental program

The following sections discuss the materials used and the shear test setup. A total of 104 samples were fabricated and tested. The bulk of the tests had three repetitions. Accordingly, a total of 36 tests with varying parameters were completed to investigate the effect of each on the overall performance of the UHPFRC panels. The test matrix (**Table 1**) included variation in the panel thickness t , connector diameter d_o , support span length l_s , edge distance c , and fiber content ρ_f .

Material properties

Connectors To understand how different connector types behave in UHPFRC, four types of cast-in connectors were tested in this study; two of these were bolt types and the other two consisted of internally threaded female inserts (**Fig. 2**). The initial connector investigated in this project was the cast-in-place zamac insert with an ultimate tensile load of 11.6 kN (2.6 kip), according to the manufacturer's data sheet. This insert, which is 25 mm (1 in.) in length and has a threaded internal diameter of 9.53 mm (0.38 in.) and an external diameter of 22.2 mm (0.87 in.), is a commercially available connector that is designed to be preinstalled in wet concrete and is known for its rust-resistant properties. Thus, it would typically be used in a wall-to-frame connection design; however, it was observed during early testing that this connection fails prematurely within the metal, making it inadequate for use in UHPC panels.

The second and third connectors are also commercially available options, namely stainless-steel L bolts and a carriage bolt with minimum tensile yield strengths of 248 and 896 MPa (36 and 130 ksi), respectively. The L bolts used varied in diameter

Table 1. Test matrix

Parameter	Variables
Connector type	Zamac insert (headed, tapered, and internally threaded), flower-shaped insert (internally threaded), L-shaped bolt (externally threaded), carriage bolt (externally threaded)
Connector diameter d_o , mm	7.94, 9.52, and 12.7
Panel thickness t , mm	15, 25, and 38
Edge distance c , mm	25, 38, 51, 64, 76, and 89
Fiber content by volume ρ_f , %	1, 2, and 3
Support span length l_s , mm	279, 330, and 381
Number of repetitions	3
Total number of tests	104
Note: 1 mm = 0.0394 in.	

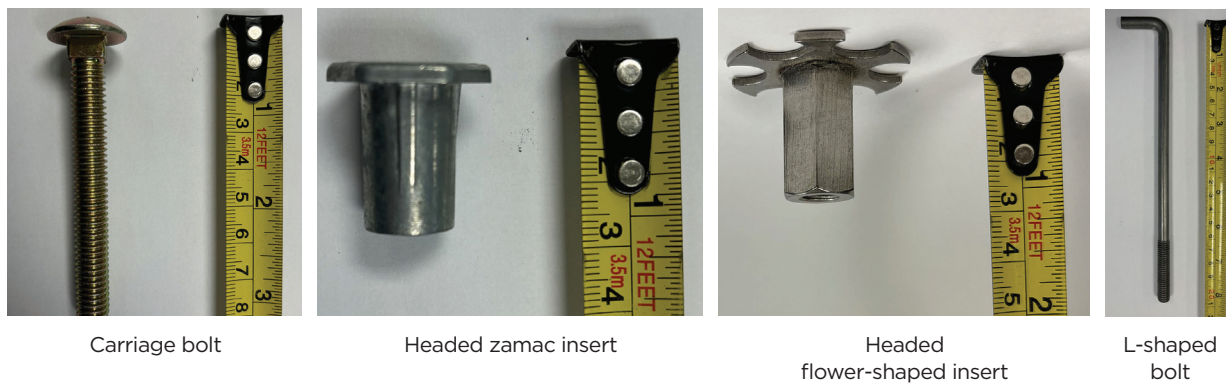


Figure 2. Connector types.

from 9.53 to 12.7 mm (0.38 to 0.5 in.) and had a hook length of 25 mm (1 in.). The carriage bolts used varied in diameter: 7.9 mm (0.3 in.), 9.53 mm, and 12.7 mm. The final connection type was an insert with external and internal threaded diameters of 13 and 7.9 mm (0.51 and 0.3 in.), respectively. They also varied in length to accommodate for the thickness of the panel they were being embedded in. The carriage bolt is labeled as a “flower” insert in this study because of the custom head shape. This insert is also commercially available and was supplied by the Canadian Precast Concrete Institute to be tested and analyzed.

Ultra-high-performance, fiber-reinforced concrete The UHPFRC was mixed using preblended material designed by the manufacturer. The concrete was self-leveling with 12 mm (0.47 in.) long polyoxymethylene (POM) fibers. These fibers had a diameter of 0.2 mm (0.008 in.) and a tensile strength of 950 MPa (138 ksi), as stated by the suppliers, and were selected over steel fibers due to their resistance to fire and inability to produce rust spots. In practice, the optimal fiber content is 2% by volume,¹⁹ which was used in this study. In this study, the fiber content was varied from 1% to 3% to determine the effect of the fiber percentage on the shear strength of connections as well as on the compressive strength of the concrete.

To determine the compressive strength of the UHPC with different fiber content, 75 × 150 mm (2.9 × 5.9 in.) concrete cylinders were tested at 28 days. It was concluded that for water-cured cylinders with 1% and 2% POM, the average compressive strengths at 28 days were 115 and 119 MPa (16.7 and 17.3 ksi) with standard deviations of 1.4 and 1.1 MPa (0.2 and 0.16 ksi), respectively. For the air-cured cylinders cast with 1%, 2%, and 3% POM fibers, the respective compressive strengths averaged 85, 109, and 89 MPa (12.3, 15.8, and 12.9 ksi) at 28 days, with standard deviations of 4.8, 14.3, and 5.6 MPa (0.7, 2.1, and 0.8 ksi), respectively. The remaining cylinders were tested at various stages to observe the change in strength over time. For the zamac insert connector that was used on a limited basis because of its consistent premature failure and poor performance, the samples were cast using

higher POM fiber content (4%) at early stages of the project. For these samples, the average compressive strength of the air-cured cylinders was 105 MPa (15.2 ksi) at 28 days with a standard deviation of 10.95 MPa (1.6 ksi).

Fabrication and specimen parameters

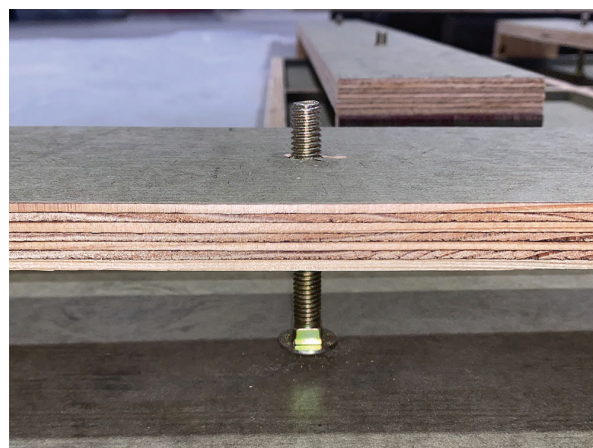
The test specimens (104 total) were fabricated using a total of six UHPFRC casts of identical mixture proportions. The parameters investigated in this study were the slab thickness t (15 to 38 mm [0.6 to 1.5 in.]), fiber content ρ (1% to 3%), connector type (carriage bolt, L bolt, cast-in-place zamac insert, and flower insert), connector diameter d_c (7.9 to 12.7 mm [0.3 to 0.5 in.]), edge distance c (25 to 89 mm [1 to 3.5 in.]), and support span (279 and 381 mm [11 and 15 in.]). The bottom edge distance below the connection was sufficiently large for all specimens to avoid pryout failure in this study. All connections were fully embedded in the panels with the head of all connectors being flush with the surface, excluding the following:

- the L bolt that had a consistent 10 mm (0.4 in.) concrete cover to avoid breakout of the connector from the backside
- the flower insert in the 38 mm (1.5 in.) thick panel that had a 13 mm (0.5 in.) concrete cover because of its limited length of 25 mm (1 in.).

The formwork was designed to have the specimens cast into individual panels that varied in size between 305 × 305 mm (12 × 12 in.), 356 × 305 mm (14 × 12 in.), and 406 × 305 mm (16 × 12 in.). The flat-headed inserts (Fig. 2) were secured to the form at their designated location using double-sided tape, whereas the carriage and L bolts were held using suspension panels connected above the forms to avoid slipping during casting (Fig. 3). The UHPFRC was mixed using a high-shear mixer and in accordance with the manufacturer’s instructions. Soaked burlap was placed over the samples with a polyethylene sheet to reduce the speed of water evaporation after pouring and were cured for 7 days after casting. After curing,



Headed insert affixed with double-sided tape



Carriage bolt aligned using suspension panels

Figure 3. Fabrication process.

the samples were removed from the formwork and stored at room temperature until they were ready to test.

Preliminary trial tests were conducted on the cast-in-place zamac insert, which was embedded at varying edge distances in UHPFRC specimens reinforced with 4% POM fibers. These tests were completed to assess the viability of this connection. It was apparent that the connection, even when embedded in its weakest panel, was not suitable for use in UHPFRC due to a consistent failure mode governed by the connector fracture.

Shear test setup

The testing frame was designed in accordance with the ASTM E488 standard²⁰ for strength of connectors in concrete members (**Fig. 4**). The aluminum frame consisted of two vertical sections on each side that were connected to two horizontal members using steel bolts and nuts. This allowed the frame to have the versatility to be adjusted in width and depth to allow for different panel sizes and thicknesses. The frame was then secured to the testing machine using four C clamps at each corner.

The concrete specimen was sandwiched between the vertical members and supported at two bearing points at its top edge. These bearing points consisted of small steel plates that were layered with neoprene to reduce the friction between the supports and the panel surface. The connector being tested was connected to a coupler, which comprised three steel plates connected to one another using threaded rods and nuts. This coupler was then connected to an eyebolt, which was fastened to the crosshead of the testing machine, guaranteeing the application of a direct shear force. The crosshead of the machine translated upward, creating a shear force on the connector, at a rate ranging from 0.75 to 1.25 mm/min (0.03 to 0.05 in./min) to ensure that the initial failure would occur within 5 minutes of testing, according to ASTM E488.²⁰ Two linear potentiom-

eters were used to accurately calculate the displacement of the connector embedded in the panel. The first one was placed on a steel angle that was connected to the coupler to measure the displacement of the connector. Another linear potentiometer was placed on a steel angle connected to the frame's vertical member to measure the elastic elongation of the aluminum frame during testing. A calibration was established to correlate vertical displacement of the frame to load. This calibration was then used to deduct frame displacement and arrive at the net vertical displacement of the connector.

Experimental results and discussion

The following sections discuss the behavior of cast-in connectors under direct shear loading. The different failure modes were detailed in addition to the ultimate shear loads that were obtained as the parameters of the panel varied. The results are summarized in **Tables 2** through **5** for the four different connector types, and failure modes are given in **Fig. 5** through **8**. There was a wide range of the ultimate shear capacity of the connectors, from 3.0 to 13.6 kN (0.7 to 3 kip), depending on the parameter being investigated.

Failure mode and general behavior

In the cases of the carriage bolt and headed insert, the failure mode was governed by a V-shaped concrete cone breakout in all cases (**Fig. 5** and **7**). This occurred regardless of the fiber content, edge distance, panel thickness, or span length. When the fiber content was increased to 3%, the samples showed a failure mode that had more random propagation in the cracks due to the increase in fibers and their random orientation within the panel. As the distance from the connector to the top free edge increased to 76 and 89 mm (3 and 3.5 in.), there was also a clear vertical split crack within the V-shaped wedge, which did not occur for panels with small edge distance.

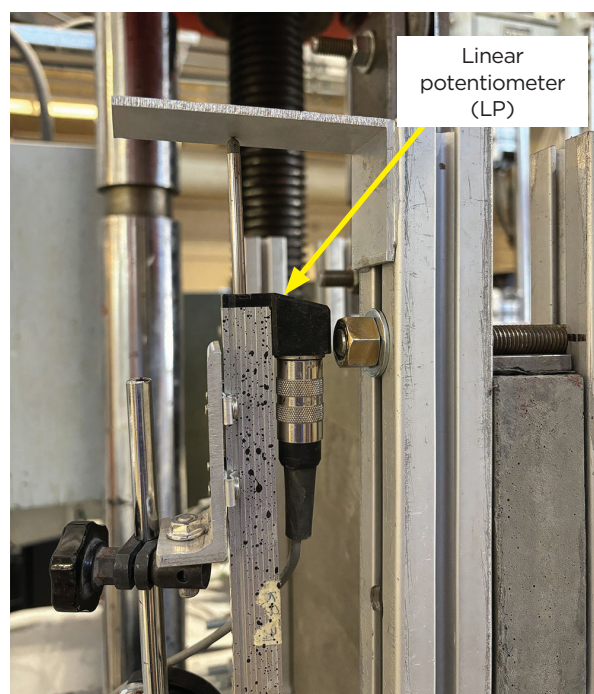
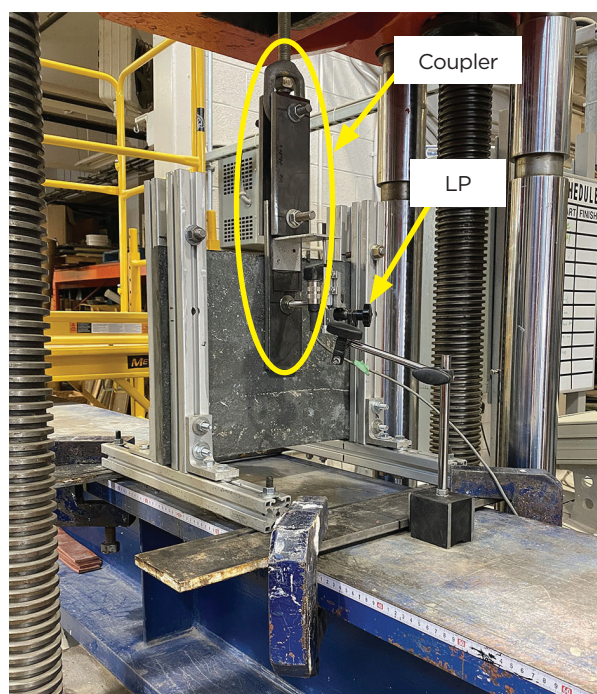
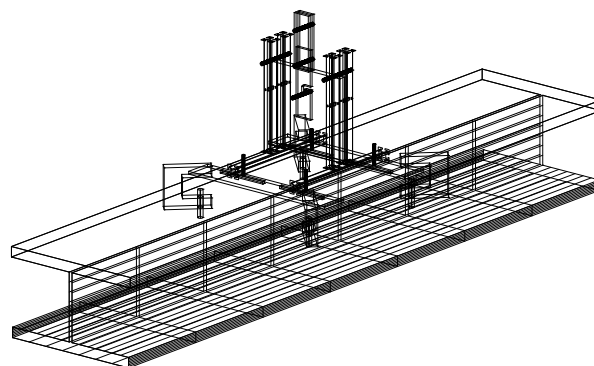
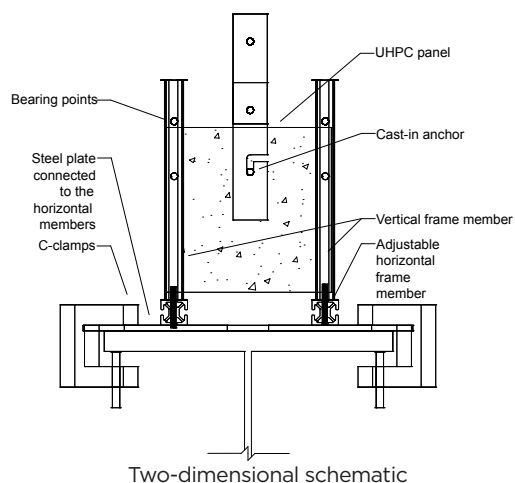


Figure 4. Shear test setup. Note: UHPC = ultra-high-performance concrete.

The panel thickness had no noticeable impact on the failure mode for the carriage bolt and flower insert in most cases. When they were embedded in the 25 and 38 mm (1 and 1.5 in.) thick panels, they would consistently form a cone breakout with the occasional vertical crack; however, in the 15 mm (0.6 in.) thick panel, they would show a cone breakout that would extend horizontally due to accidental eccentricity during testing. In addition, a change in the diameter of the bolt showed no impact on the failure mode of the panels.

The L bolt behaved differently compared with the former connector types. Due to the geometry of the connector, the failure

mode during testing was consistently governed by the connector rather than the concrete (Fig. 6). Even when placed in its weakest panel, the result would regularly show minor thin hairline cracks followed by clear connector yielding. There was only one particular case that showed a full concrete breakout, which is attributed to the diameter of the L bolt being increased from 9.5 to 12.7 mm (0.4 to 0.5 in.). The increase in the diameter of the bolt allowed it to have a higher shear capacity compared with the smaller diameter, which resulted in a concrete breakout.

The specimens cast with the zamac insert regularly displayed clear connector failure (Fig. 8) by shearing the head

Table 2. Carriage bolt experimental shear results

Test number	d_o , mm	t , mm	Fiber content, %	Slab size, mm	l_s , mm	l , mm	c , mm	V_u , kN	Average V_u , kN	Standard deviation, kN	COV	Failure mode
1	7.9	15	2	406 × 305	381	15	89	6.9	6.0	0.67	0.11	CCB
		15.5						5.3				CCB
		14						5.7				CCB
2	7.9	24	2	356 × 305	330	25	76	9.5	9.4	0.16	0.02	CCB
		25						9.2				CCB
		25.5						9.5				CCB
3	9.5	14	2	356 × 305	330	15	76	5.1	5.5	0.36	0.07	CCB
		13.5						5.9				CCB
		13.5						5.5				CCB
4	9.5	15	2	406 × 305	381	15	76	4.9	5.0	0.12	0.02	CCB
		14						5.0				CCB
		14						5.2				CCB
5	9.5	24.5	2	305 × 305	279	25	25	3.7	3.9	0.36	0.09	CCB
		25						4.4				CCB
		24						3.6				CCB
6	9.5	25	2	305 × 305	279	25	38	4.2	4.4	0.12	0.03	CCB
		25						4.4				CCB
		25						4.5				CCB
7	9.5	25	2	305 × 305	279	25	51	6.1	6.3	0.18	0.03	CCB
		25						6.6				CCB
		23						6.3				CCB
8	9.5	24	2	305 × 305	279	25	64	6.7	6.5	0.49	0.08	CCB
		21						5.8				CCB
		23						6.9				CCB
9	9.5	25	2	356 × 305	330	25	76	9.3	8.6	0.44	0.05	CCB
		25						8.3				CCB
		24						8.4				CCB
10	9.5	24	2	406 × 305	381	25	76	9.1	8.8	0.22	0.03	CCB
		22						8.6				CCB
		24						8.7				CCB
11	9.5	23	2	406 × 305	381	25	89	9.3	8.8	0.48	0.05	CCB
		23						8.3				CCB
12	9.5	25	1	305 × 305	279	25	64	5.8	6.5	0.93	0.14	CCB
		24						5.9				CCB
		26						7.8				CCB

continued on p. 32

Table 2. Carriage bolt experimental shear results (continued from p. 31)

Test number	d_o , mm	t , mm	Fiber content, %	Slab size, mm	l_s , mm	l , mm	c , mm	V_u , kN	Average V_u , kN	Standard deviation, kN	COV	Failure mode
13	9.5	25	3	305 × 305	279	25	64	10.4	9.9	0.52	0.05	CCB
		25						10.0				CCB
		25						9.2				CCB
14	12.7	25	2	356 × 305	330	25	76	11.6	10.4	1.20	0.12	CCB
		23						10.8				CCB
		23						8.7				CCB
15	9.5	37	2	356 × 305	330	38	76	11.9	11.9	0.50	0.04	CCB
		37						11.3				CCB
		38						12.5				CCB
16	9.5	35	2	406 × 305	381	38	76	9.4	10.9	1.37	0.13	CCB
		38						12.7				CCB
		35						10.4				CCB

Note: CCB = concrete cone breakout; COV = coefficient of variation; c = edge distance; d_o = nominal connector diameter; l = embedment depth; l_s = support span length; t = panel thickness; V_u = ultimate shear load. 1 mm = 0.0394 in.; 1 kN = 0.225 kip.

of the insert off. In specific cases where the connector was located close to the edge, there was a combination of connector failure and concrete cone breakout.

Effect of connector diameter

Figure 9 plots the average ultimate shear load obtained for the carriage and L bolts with respect to the diameters of these connections. The carriage bolts were embedded in 25 mm (1 in.) thick panels reinforced with 2% POM. As the diameter of the carriage bolt increased from 7.9 to 12.7 mm (0.3 to 0.5 in.), the load increased by 10%, from 9.4 to 10.3 kN (2.1 to 2.3 kip) due to the increase in the load-bearing area being controlled by the diameter.

Figure 9 also plots the shear capacity for the 9.5 and 12.7 mm (0.4 and 0.5 in.) diameter L bolts embedded in a 38 mm (1.5 in.) thick panel reinforced with 2% POM. There was a 64% increase in strength, from 7.7 to 12.6 kN (1.7 to 2.8 kip), as the diameter of the L bolt increased from 9.5 to 12.7 mm. The justification for this increase is primarily due to the failure mode for the panels, with 9.5 mm L bolts being controlled by the connector rather than the UHPC. This resulted in a lower shear capacity. For the panels that had a 12.7 mm L bolt diameter, the failure mode was governed by the concrete and formed a concrete cone breakout at failure. This allowed the concrete to reach its full capacity, resulting in a higher overall shear capacity.

Figure 9 shows the load-displacement response of carriage bolts of different diameters. An initial nearly linear response can be seen until the peak load is reached. The load then

drops gradually because of the fibers as they control the rate of crack opening. Both connector diameters also showed considerable and comparable deformations after the samples had reached the peak load.

Effect of connector type

A comparison between the connector types with matching parameters was also investigated. **Figure 10** compares the load-displacement responses of samples of different connection types. Figure 10 compares the carriage bolt that had a diameter of 12.7 mm (0.5 in.) and the headed flower insert that had a similar external diameter of approximately 13 mm (0.5 in.), both with a UHPC panel thickness of 25 mm (1 in.) and connector edge distance of 76 mm (3 in.). Figure 10 also shows that both types had a similar strength and overall behavior. A similar result was shown when a 12.7 mm diameter L bolt was compared to the flower insert of 13 mm outer diameter in a 38 mm (1.5 in.) thick panel. Moreover, Fig. 10 shows that changing the shape of the connectors had no influence on the shear strength and ductility of the panel, provided that the diameter of the connector in contact with concrete is similar.

Effect of POM fiber content

Figure 11 presents the effect of fiber content on the shear capacity and behavior of the connectors. This study investigated a variation in POM fiber content from 1% to 3% for the carriage bolt and flower insert in panels that were 25 and 15 mm (1 and 0.6 in.) thick, respectively. For a connector placed 64 mm (2.5 in.) from the free edge, the

Table 3. L-shaped bolt experimental shear results

Test number	d_o , mm	t , mm	Fiber content, %	Slab size, mm	l_s , mm	l , mm	c , mm	V_u , kN	Average V_u , kN	Standard deviation, kN	COV	Failure mode
1	9.5	24	2	356 × 305	330	15	76	7.9	8.3	0.38	0.05	CF/TC
		25						8.8				CF/TC
		27						8.2				CF/TC
2	9.5	26	2	406 × 305	381	15	76	8.7	8.5	0.21	0.02	CF/TC
		25						8.2				CF/TC
		25						8.5				CF/TC
3	9.5	38	2	305 × 305	279	28	38	6.6	6.2	0.63	0.10	CF/TC
		36						6.7				CF/TC
		36						5.3				CF/TC
4	9.5	38	2	305 × 305	279	28	51	6.9	7.5	0.44	0.06	CF/TC
		37						7.9				CF/TC
		37						7.8				CF/TC
5	9.5	34	2	305 × 305	279	28	64	7.9	7.9	0.05	0.01	CF/TC
		35						7.9				CF/TC
		37						8.0				CF/TC
6	9.5	40	2	356 × 305	330	28	76	7.2	7.7	0.36	0.05	CF
		40						7.9				CF
		38						7.9				CF
7	9.5	36	2	406 × 305	381	28	76	7.2	7.6	0.34	0.04	CF
		35						7.9				CF
		37						7.8				CF
8	12.7	38	2	356 × 406	330	28	76	12.2	12.6	0.35	0.03	CCB
		37						12.6				CCB
		40						13.1				CCB

Note: CCB = concrete cone breakout; CF = connector failure; COV = coefficient of variation; c = edge distance; d_o = nominal connector diameter; l = embedment depth; l_s = support span length; t = panel thickness; TC = thin hairline cracks; V_u = ultimate shear load. 1 mm = 0.0394 in.; 1 kN = 0.225 kip.

carriage bolt showed no increase in strength from 1% to 2% POM fiber content. The average remained at a constant of 6.5 kN (1.5 kip); however, there was a 52% increase in strength, from 6.5 to 9.9 kN (1.5 to 2.2 kip), when the fiber content increased from 2% to 3%. A similar growth of 53% was shown for the flower insert as the fiber content was increased from 2% to 3%, with a small effect when it increased from 1% to 2%. Increasing the fiber content to 3% also showed a noticeable effect on the load-displacement responses, with significant increases in ductility and progressive failure compared with the samples with 1% and 2% fiber content due to the crack bridging of the fibers. A similar observation was reported for postinstalled connectors.¹⁷

Effect of UHPC panel thickness

Figure 12 displays the effect of panel thickness on ultimate shear strength and load-displacement responses. All of these tests consisted of connectors that were fully embedded in panels cast with 2% POM fibers. The carriage bolt tests were 9.53 mm (0.375 in.) in diameter and located 76 mm (3 in.) from the edge, whereas the flower insert tests were all 7.9 mm (0.3 in.) insert diameters and were also at an edge distance of 76 mm. Increasing the thickness of the plate from 15 to 25 mm (0.6 to 1 in.) resulted in average increases of 57% and 62% for the carriage bolt and flower insert, respectively. This is consistent with the ACI 318-19 design provisions, which state that the ultimate shear capacity of

Table 4. Flower-shaped insert experimental shear results

Test number	d_o , mm	t , mm	Fiber content, %	Slab size, mm	l_s , mm	l , mm	c , mm	V_u , kN	Average V_u , kN	Standard deviation, kN	COV	Failure mode
1	7.9	13	2	305 × 305	279	15	25	3.6	3.4	0.28	0.08	CCB
		15						3.0				CCB
		14						3.5				CCB
2	7.9	14	2	305 × 305	279	15	51	3.7	4.0	0.88	0.22	CCB
		13						5.3				CCB
		15						3.2				CCB
3	7.9	14	2	305 × 305	279	15	64	4.2	5.1	0.60	0.12	CCB
		14						5.6				CCB
		14						5.3				CCB
4	7.9	16	1	305 × 305	279	15	64	4.5	4.5	0.13	0.03	CCB
		15						4.6				CCB
		15						4.3				CCB
5	7.9	16	3	305 × 305	279	15	64	7.5	7.8	1.08	0.14	CCB
		17						9.2				CCB
		15						6.6				CCB
6	7.9	14	2	356 × 305	330	15	76	6.9	6.4	0.78	0.12	CCB
		16						7.1				CCB
		14						5.4				CCB
7	7.9	25	2	356 × 305	330	25	76	10.8	10.5	0.53	0.05	CCB
		25						10.8				CCB
		23						9.7				CCB
8	7.9	39	2	356 × 305	330	25	76	12.7	12.8	0.49	0.04	CCB
		37						12.3				CCB
		37						13.4				CCB

Note: CCB = concrete cone breakout; COV = coefficient of variation; c = edge distance; d_o = nominal connector diameter; l = embedment depth; l_s = support span length; t = panel thickness; TC = thin hairline cracks; V_u = ultimate shear load. 1 mm = 0.0394 in.; 1 kN = 0.225 kip.

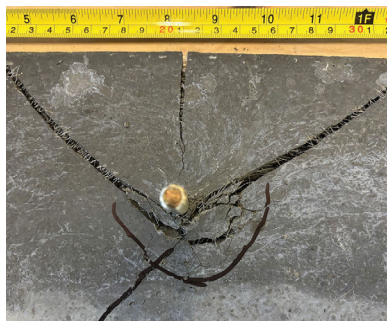
Table 5. Zamac insert experimental shear results

Test number	d_o , mm	t , mm	Fiber content, %	Slab size, mm	l_s , mm	l , mm	c , mm	V_u , kN	Average V_u , kN	Standard deviation, kN	COV	Failure mode
1	9.5	25	4	305 × 305	279	25	25	5.4	6.6	1.0	0.15	CF/CCB
		26						7.9				CF/CCB
		25						6.7				CF/CCB
2	9.5	23	4	305 × 305	279	25	38	10.1	10.7	0.57	0.05	CF/CCB
		27						11.3				CF/CCB
3	9.5	26	4	305 × 305	279	25	60	13.2	13.9	0.70	0.05	CF/TC
		26						14.6				CF/TC
4	9.5	25	4	305 × 305	279	25	76	13.5	13.6	0.05	0.01	CF/TC
		26						13.6				CF/TC

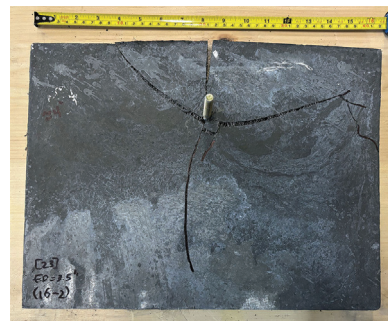
Note: CCB = concrete cone breakout; CF = connector failure; COV = coefficient of variation; c = edge distance; d_o = nominal connector diameter; l = embedment depth; l_s = support span length; t = panel thickness; TC = thin hairline cracks; V_u = ultimate shear load. 1 mm = 0.0394 in.; 1 kN = 0.225 kip.



Cone breakout



Close-up showing fiber breakage and vertical concrete split

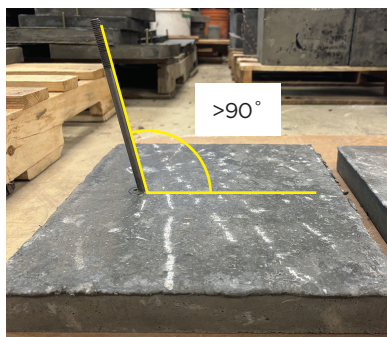


Asymmetric concrete cone breakout with downward vertical cracks

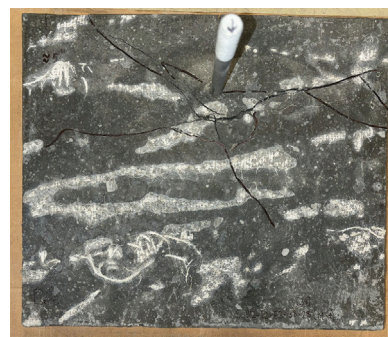
Figure 5. Carriage bolt failure modes and cracking pattern.



Minor concrete cracking



Bending in the bolt

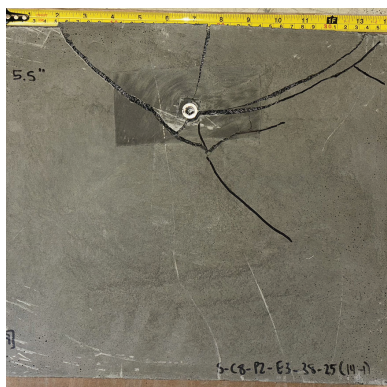


Horizontal and radial concrete cracking

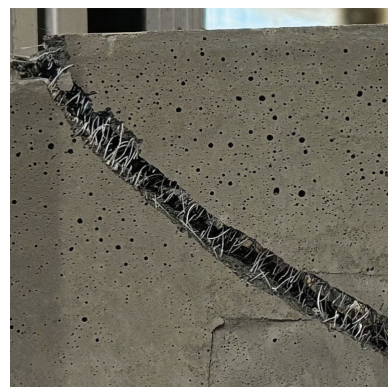
Figure 6. L-shaped bolt failure modes. Note: 1° = 1 degree.



Backside punching effect



Concrete cone breakout



Close-up of fiber breakage

Figure 7. Flower-shaped insert failure modes.



Failed connector with the attached threaded rod



Minor concrete cracking

Figure 8. Zamac insert failure modes.

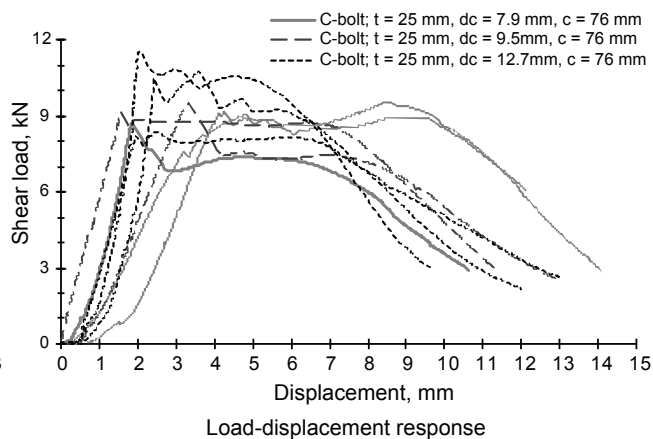
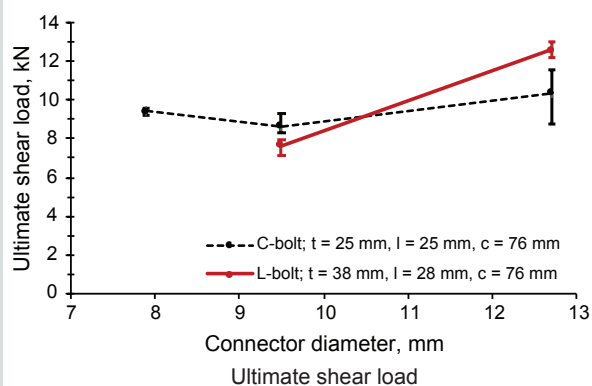


Figure 9. Effect of connector diameter on shear strength. Note: c = edge distance to the free edge; C-bolt = carriage bolt; d_c = connector diameter; L-bolt = L-shaped bolt; t = panel thickness. 1 mm = 0.0394 in.; 1 kN = 0.225 kip.

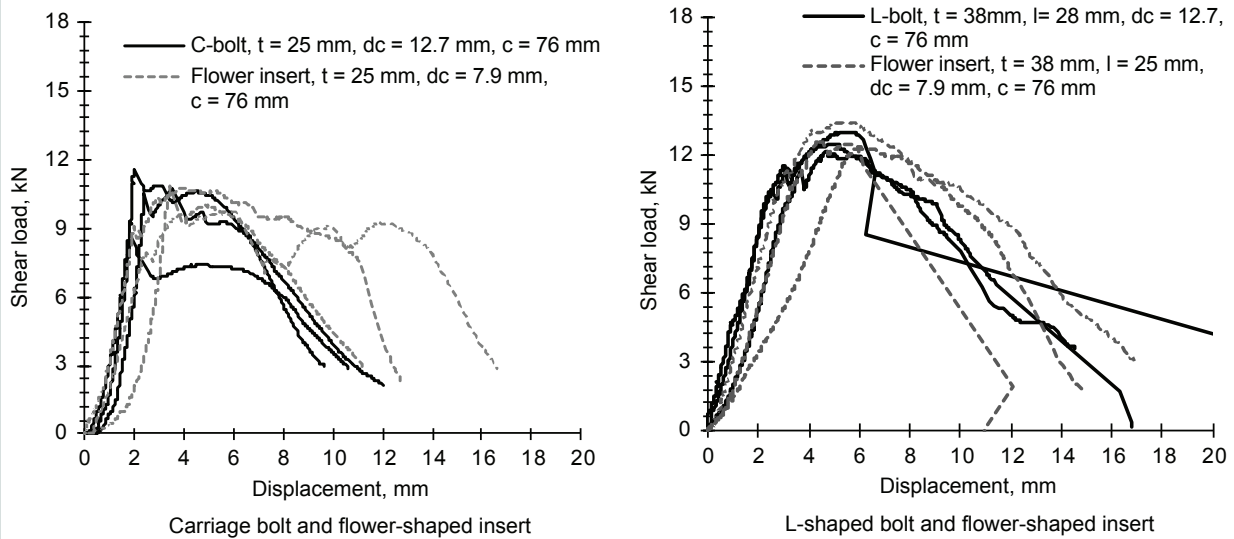


Figure 10. Load-displacement curves for connectors with similar diameters. Note: c = edge distance to the free edge; C-bolt = carriage bolt; d_c = connector diameter; L-bolt = L-shaped bolt; t = panel thickness. 1 mm = 0.0394 in.; 1 kN = 0.225 kip.

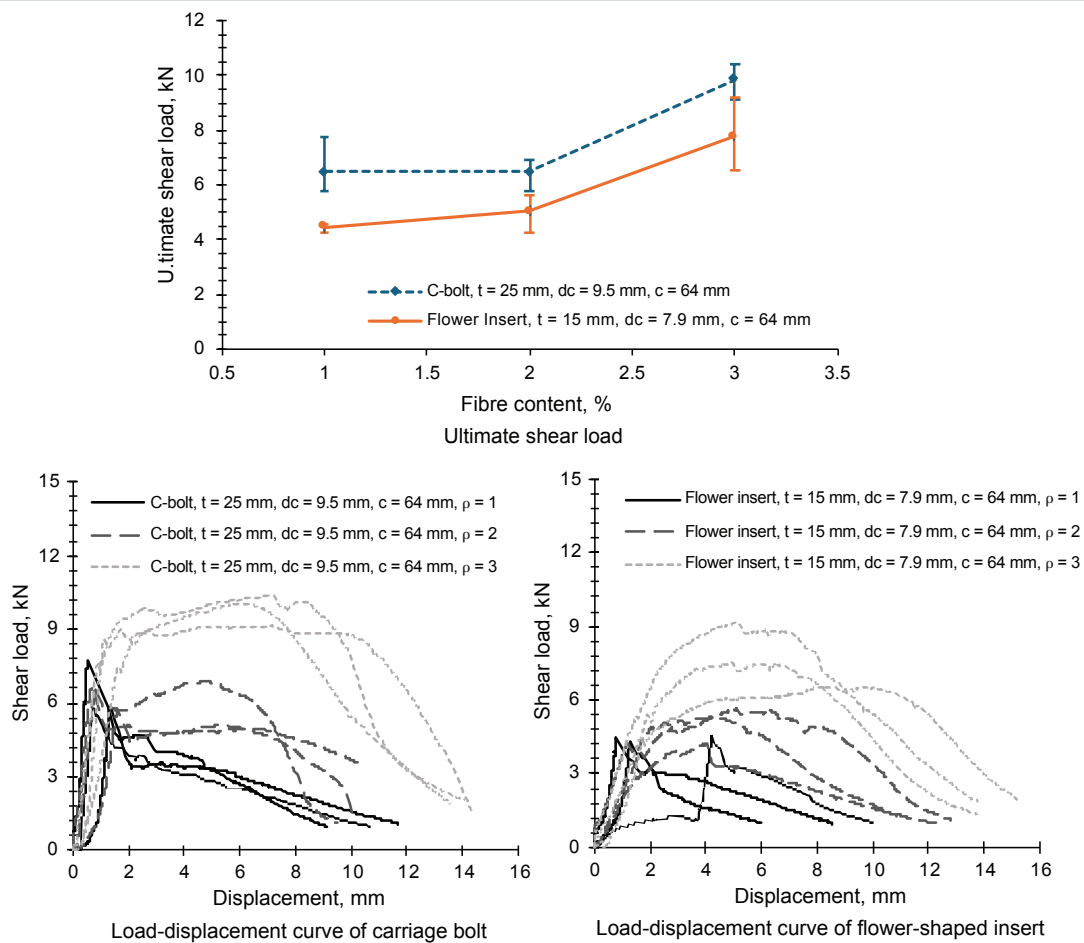


Figure 11. Effect of POM fiber content on shear strength. Note: c = edge distance to the free edge; C-bolt = carriage bolt; d_c = connector diameter; POM = polyoxymethylene; t = panel thickness; ρ = fiber content. 1 mm = 0.0394 in.; 1 kN = 0.225 kip.

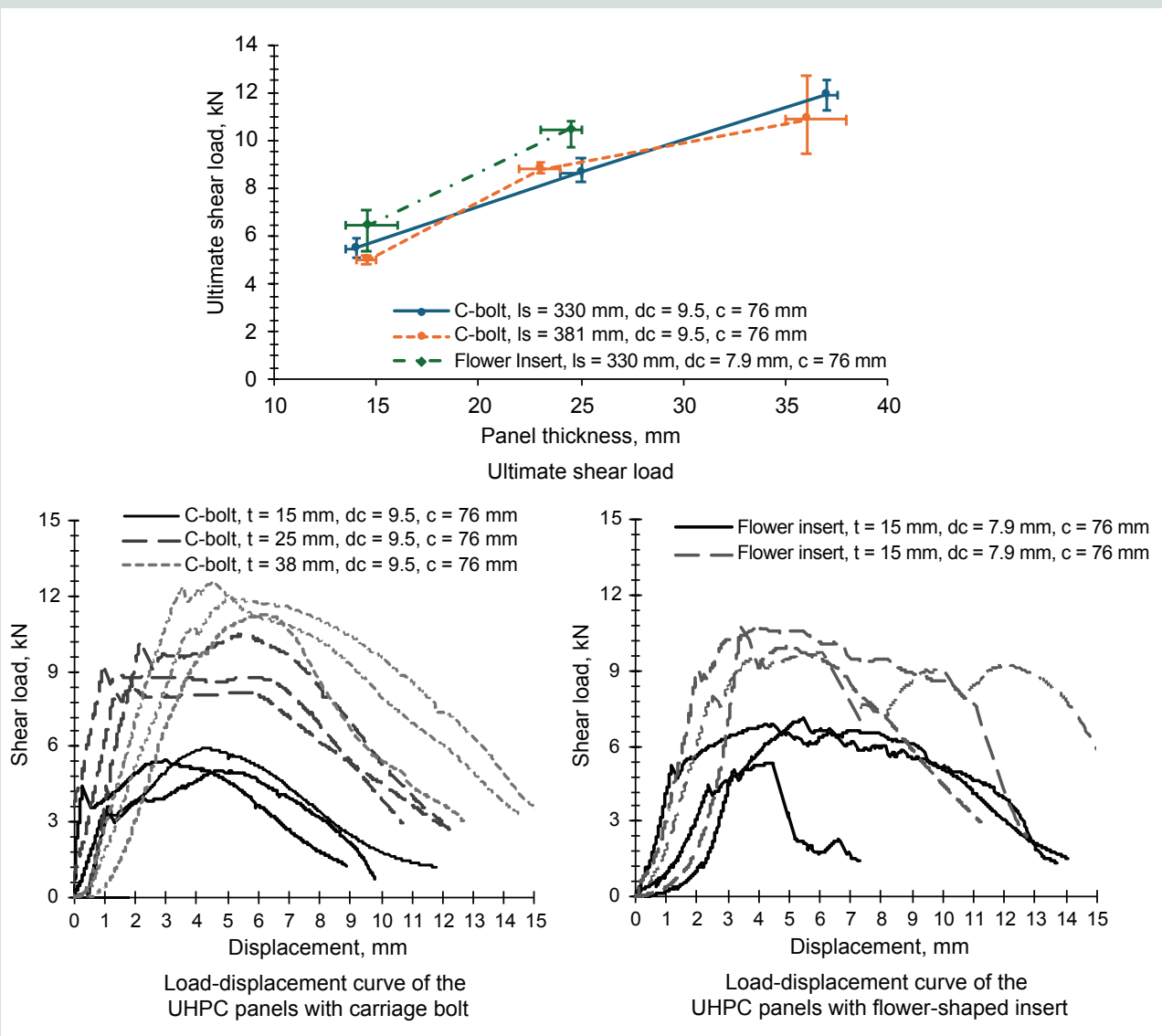


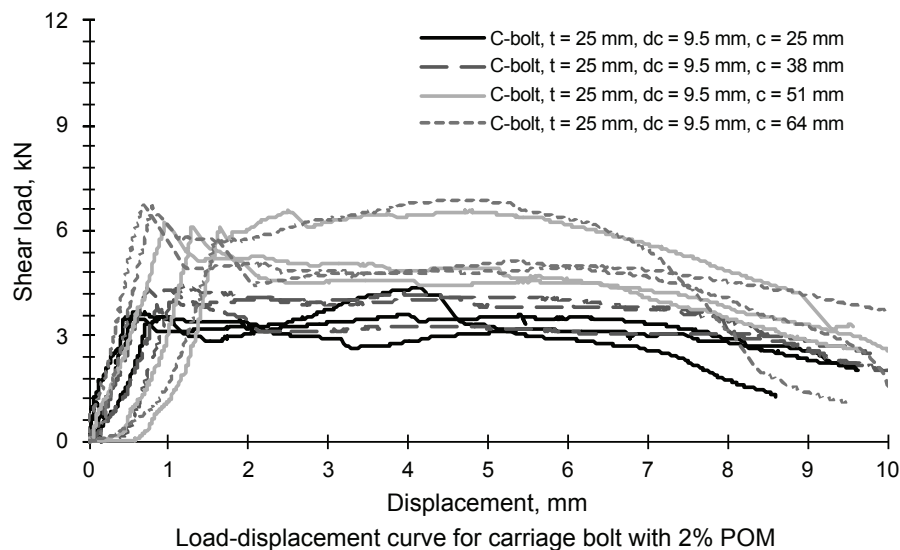
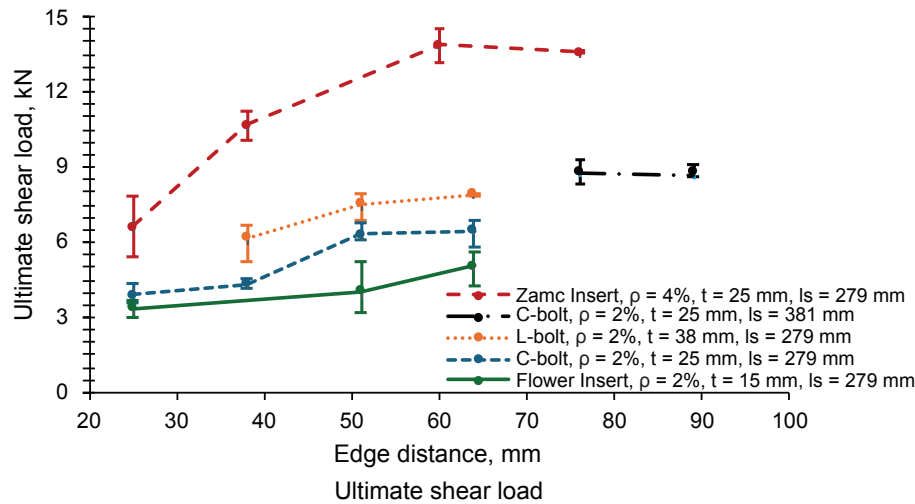
Figure 12. Effect of panel thickness on shear strength. Note: c = edge distance to the free edge; C-bolt = carriage bolt; d_c = connector diameter; l_s = support span length; t = panel thickness; UHPC = ultra-high-performance concrete. 1 mm = 0.0394 in.; 1 kN = 0.225 kip.

the anchor is proportional to the load-bearing length of the anchor in the panel, which in this case is the embedment depth of the connector. Furthermore, an increase in the thickness of the panel from 25 to 38 mm (1 to 1.5 in.) resulted in an average capacity increase of 38% for the carriage bolt. Figure 12 also shows the load-displacement curves for different panel thicknesses for carriage bolt and flower inserts, respectively. Both load and deflections increased with panel thickness. All panels experienced a consistent failure mode of concrete breakout.

Effect of edge distance

Figure 13 shows the effect of edge distance on shear strength and load-displacement response. As the edge distance was increased, the shear strength also increased for all four connectors. For the carriage bolt, and based on

a consistent concrete cone breakout failure, the strength stabilized at 76 mm (3 in.) edge distance when the accompanying concrete cone breakout no longer occurred. Between 25 and 76 mm (1 to 3 in.) edge distance, the load increased 2.25 times and then seemed to plateau when the edge distance increased from 76 to 89 mm (3 to 3.5 in.). Similarly, the increase in edge distance for the L bolt from 38 to 64 mm (1.5 to 2.5 in.) and the increase for the flower insert from 25 to 64 mm (1 to 2.5 in.) resulted in strength increases of 29% and 51%, respectively. Increasing the edge distance of the zamac insert from 25 to 60 mm (1 to 2.4 in.) caused an increase in shear strength of 2.1 times, where failure occurred by fracture of the connector combined with concrete cone breakout. The strength stabilized beyond the edge distance of 60 mm as failure was governed by fracture of the insert only, without concrete cracking. The load-displacement responses of the carriage bolt at various edge



Load-displacement curve for carriage bolt with 2% POM

Figure 13. Effect of edge distance of connector on shear strength. Note: c = edge distance to the free edge; C-bolt = carriage bolt; d_c = connector diameter; l_s = support span length; L-bolt = L-shaped bolt; POM = polyoxymethylene; t = panel thickness; ρ = fiber content. 1 mm = 0.0394 in.; 1 kN = 0.225 kip.

distances in Fig. 13 were all similar but are scaled up or down in load depending on edge distance.

Effect of support span length

Figure 14 shows the impact of the support span length, namely 330 and 381 mm (13 and 15 in.), on the ultimate shear strength and load-displacement responses. All samples had the same connector diameter, fiber content, and edge distance. Increasing the span length from 330 to 381 mm resulted in insignificant change in shear strengths, ranging from +2% to -9% for different panel thicknesses. This is consistent with Prejs, Jawdhari, and Fam,¹⁷ who also observed a negligible effect of the support span length on the shear capacity of postinstalled connectors when varying different span lengths ranging from 178 to 279 mm (7 to 11 in.). A similar observation was made for a variation in the support span for the L bolts embedded in 25 and 38

mm (1 and 1.5 in.) thick panels, which shows the load-displacement responses of various panels.

ASTM E488²⁰ states that the spacing between the test supports needs to be a minimum of four times the edge distance. This ensures that the failure of the member will be in between the two supports without being influenced by them. Because all samples satisfied this requirement, increasing the support length resulted in a minor influence on the results.

Design equations

This section compares the experimental data obtained for all connector types with the predictions using existing models. A modification of the design equation for shear strength of cast-in connectors is presented.

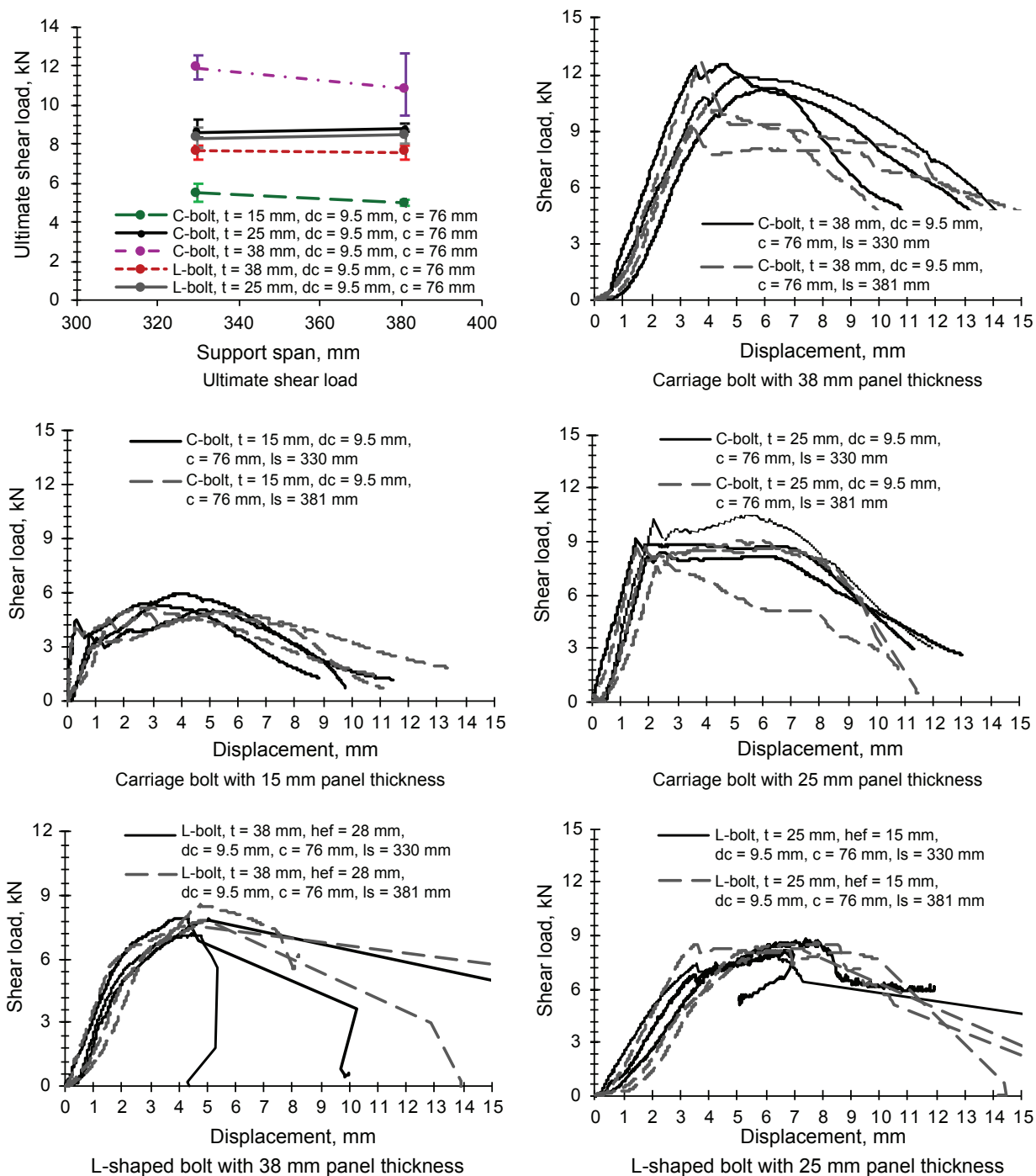


Figure 14. Effect of support span length on shear strength and load-displacement curves. Note: c = edge distance to the free edge; C-bolt = carriage bolt; d_c = connector diameter; l_s = support span length; L-bolt = L-shaped bolt; t = panel thickness. 1 mm = 0.0394 in.; 1 kN = 0.225 kip.

Existing shear strength prediction models

ACI 318-19 states that for a single connector in normal-strength concrete, its basic concrete breakout shear strength should not exceed the lesser of Eq. (1) and (2). Based

on the parameters of this study, Eq. (1) consistently governed. **Figure 15** plots the experimental versus the predicted ultimate shear loads using Eq. (1). Generally, the graph shows that the ACI equation, which is for normal-strength concrete, significantly overestimated the capacity of the cast-in-place connectors in thin UHPC panels. The graph also shows the

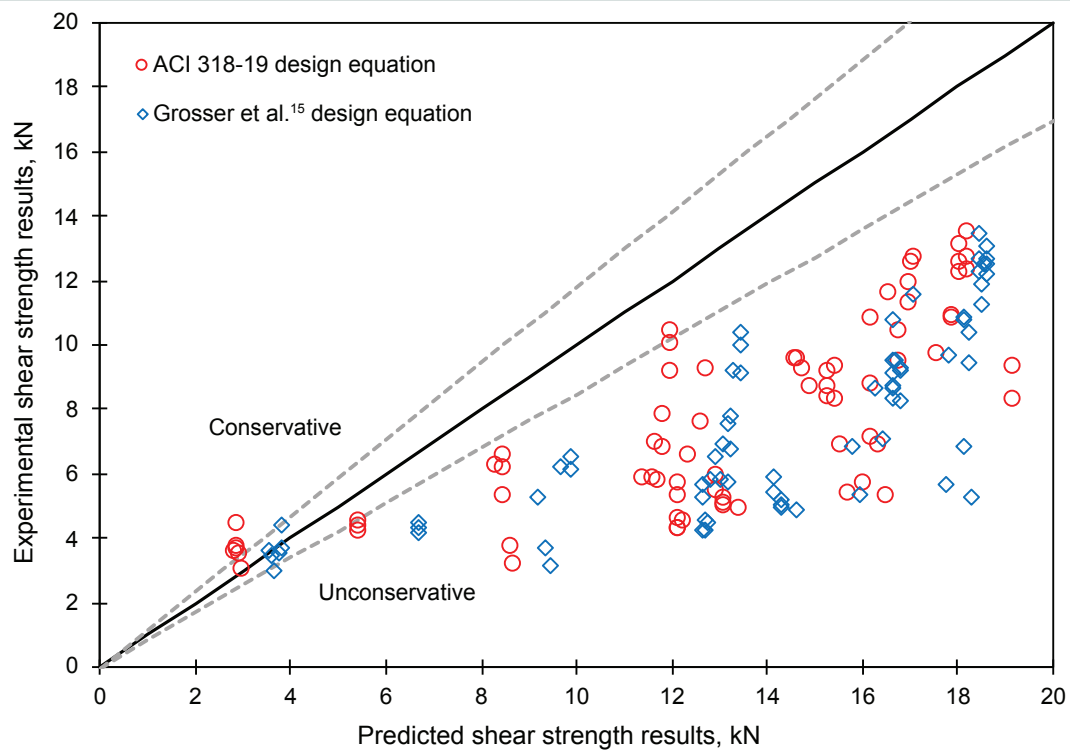


Figure 15. Predicted versus experimental shear strength of cast-in-place anchors in thin UHPC panels using existing design equations for cast-in anchors in conventional concrete panels. Note: UHPC = ultra-high-performance concrete. 1 kN = 0.225 kip.

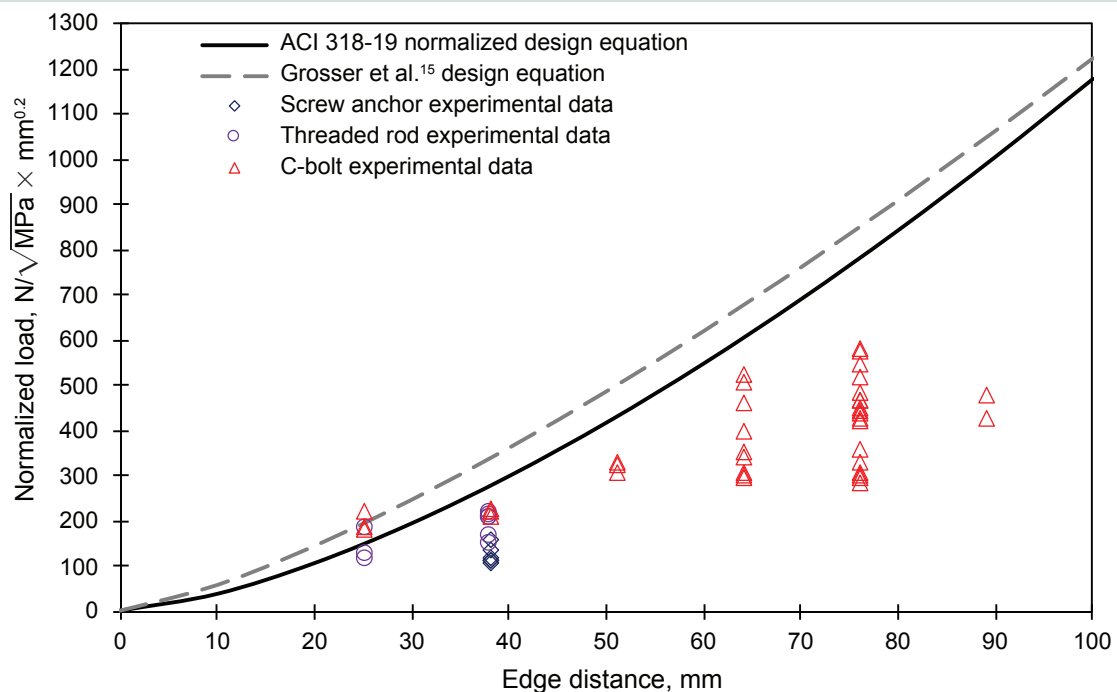


Figure 16. Effect of edge distance on normalized shear strength for 9.53 mm diameter carriage bolt cast-in-place connectors (this study) and two types of postinstalled connectors¹⁷ in thin UHPC panels. Source: Data from Choi, Joh, and Chun (2015). Note: C-bolt = carriage bolt; UHPC = ultra-high-performance concrete. 1 mm = 0.0394 in.

predictions of the Grosser et al.¹⁵ Equation (3) for cast-in-place connectors in normal-strength concrete, which also significantly overestimated strength.

Figure 16 presents the effect of edge distance on normalized shear strength of the cast-in-place 9.53 mm (0.375 in.) carriage bolts in this study as well as comparably sized postinstalled connectors¹⁷ in thin UHPC panels with POM fibers. The results are presented in reference to the ACI 318-19 and the Grosser et al.¹⁵ equations. Figure 16 shows that the equations continually overestimated the ultimate shear capacity, with an inconsistent difference between the predicted and experimental data, which suggests that it is not possible to introduce a simple modification to these equations.

Figure 17 shows the predicted shear strength of the cast-in-place connectors in this study using existing equations for UHPC. Eq. (4) and (5) were proposed by Prejs, Jawdhari, and Fam¹⁷ for two types of postinstalled connectors in thin UHPC with POM fibers, namely threaded rods and screw connectors. Figure 17 shows that these equations significantly underestimated the strength of the cast-in connectors. Also, Choi, Joh, and Chun¹⁸ proposed Eq. (6) for cast-in-place connectors in thick (100 mm [(4 in.)] UHPC panels with steel fibers. Figure 17 shows that this equation overestimated the strength of the connectors, which stems from the equation being derived for use on thick UHPC panels reinforced with steel fibers.

Proposed design equation

The trend of the Prejs, Jawdhari, and Fam¹⁷ equations in Fig. 17 suggests the possibility of a simple modification using a single multiplier to adjust the equation from applicability in postinstalled to cast-in-place connectors, specifically in Eq. (5). Equation (5), representing the threaded rod design equation, underestimated the capacity of the cast-in-place connectors consistently by a factor of 0.6 with a coefficient of variation of 0.14. Integrating this factor into the design equation allows for a more accurate representation of the cast-in-place connection strength in thin UHPC panels. This changes the design equation factor in Eq. (5) to 2.25 instead of 1.35 by multiplying the original postinstalled factor by 1.7, which results in 85% of the experimental data points fitting into a 15% error range (**Fig. 18**). Equation (7) is developed for cast-in-place connectors in thin UHPFRC panels ranging from 15 to 38 mm (0.6 and 1.5 in.) in thickness, connector diameters ranging from 7.9 to 12.7 mm (0.3 to 0.5 in.), edge distances of up to 89 mm (3.5 in.), and POM fiber content ranging from 1% to 3%.

$$V_u = 2.25 \times 10^{-3} l^{0.71} d_o^{0.03} \rho_f^{0.36} \sqrt{f'_c} c^{0.8} \quad (7)$$

Conclusion

This study investigated the shear strength and behavior of two types of cast-in connectors, namely inserts and bolts, in

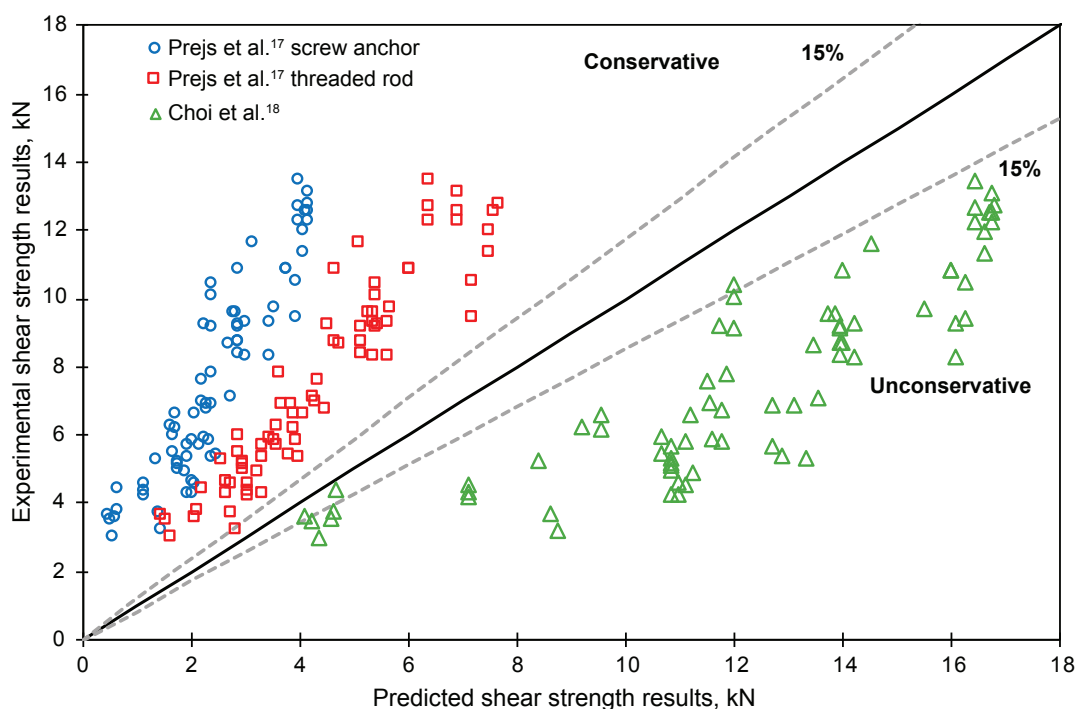


Figure 17. Predicted versus experimental shear strength of cast-in-place anchors in thin UHPC panels using existing design equations for anchors in UHPC. Note: UHPC = ultra-high-performance concrete. 1 kN = 0.225 kip.

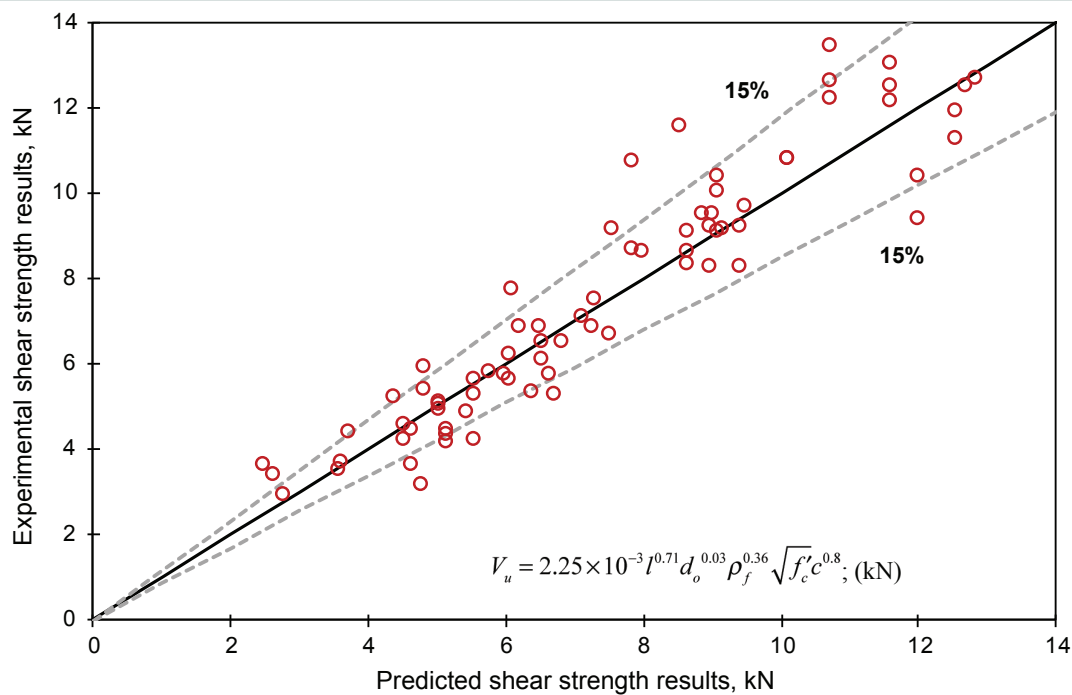


Figure 18. Predicted versus experimental ultimate shear strength for cast-in-place connectors in thin UHPC panels with POM fibers using a modified design equation. Note: c = edge distance to the free edge; d_o = outer diameter of connector; f'_c = concrete compressive strength; l = embedment (bearing) length; POM = polyoxymethylene; UHPC = ultra-high-performance concrete; V_u = concrete breakout shear capacity; ρ_f = fiber content by volume. 1 kN = 0.225 kip.

thin UHPC panels with POM fibers. The parameters investigated were insert and bolt type and diameter, POM fiber content, UHPC panel thickness, edge distance of connector, and support span of panel. The two inserts studied were a flower-shaped headed insert and a headed conical (zamac) insert with inner threaded central holes. The two bolts studied were a threaded headed carriage bolt and an L bolt. The study compared the cast-in-place connectors with postinstalled ones of equivalent size and panels. The applicability of existing design equations to these types of connectors was also investigated. The following conclusions were drawn:

- Cast-in-place connectors outperformed the postinstalled threaded rod connectors (installed through holes in the panel and anchored from both sides) in all scenarios by a factor of 1.7 in terms of shear strength. This was consistent for various parameters.
- The failure modes of the carriage bolt and flower insert were governed by concrete cone breakout in all cases. As edge distance increased, additional vertical splitting cracks occurred. L bolts failed by yielding of the bolt, except for the largest (12.7 mm [0.5 in.]) bolt, where concrete cone breakout failure occurred. All zamac inserts experienced brittle fracture of the insert.
- The shape and type of cast-in-place connectors of the same size had a trivial effect on shear strength and ductility.
- Increasing carriage bolt diameter had an insignificant effect on shear strength (for example, only a 10% increase when diameter increased from 9.5 to 12.7 mm [0.4 to 0.5 in.]). For the same diameter increase, the shear strength of L bolts increased 64% because the failure mode changed from steel yielding of the bolt to concrete cone breakout failure.
- The increase of POM fiber content from 1% to 2% had little effect on shear strength; however, when POM fiber content was increased from 2% to 3%, there was a 52% increase in strength. A noticeable effect on the load-displacement response and ductility was also observed compared with the 1% and 2% fiber content.
- Shear strength was directly proportional to panel thickness. Increasing panel thickness from 15 to 38 mm (0.6 to 1.5 in.) resulted in a 100% increase in shear strength.
- Increasing the edge distance of the anchor from 25 to 64 mm (1 to 2.5 in.) resulted in an average increase of 66% in shear capacity but had no effect on the ductility of the panel.
- Shear strength design equations for cast-in-place connectors in normal-strength concrete, such as in ACI 318-19, grossly overestimate the shear strength of cast-in-place connectors in thin UHPC panels by up to 200%.

Shear strength design equations for postinstalled threaded rod or screw connectors in thin UHPC panels with POM fibers¹⁷ grossly underestimated the capacity of the cast-in-place connectors; however, a direct correlation was established through a factor of 1.7, which was relatively consistent across the full range of shear loads. This was the basis for the new proposed design equation for cast-in-place connectors based on modifying the Prejs, Jawdhari, and Fam¹⁷ equation. Although the modification to the design equation showed promise in estimating the shear capacity of cast-in connectors in thin UHPC panels, further verification is required to validate the newly proposed equation for a full-scale sandwich panel. Further investigation is essential to show the behavior of these connections under different boundary conditions to better simulate the real-life behavior of cast-in connectors in thin precast UHPC panels.

Acknowledgments

The authors wish to acknowledge the contributions of the Canadian Precast/Prestressed Concrete Institute, ceEntek North America, and the MITACS Accelerate program to this project.

References

1. Akça, K. R., and M. İpek. 2022. "Effect of Different Fiber Combinations and Optimisation of an Ultra-High Performance Concrete (UHPC) Mix Applicable in Structural Elements." *Construction and Building Materials*, no. 315, 125777. <https://doi.org/10.1016/j.conbuildmat.2021.125777>.
2. Akeed, M. H., S. Qaidi, H. U. Ahmed, R. H. Faraj, A. S. Mohammed, W. Emad, B. A. Tayeh, and A. R. G. Azevedo. 2022. "Ultra-High-Performance Fiber-Reinforced Concrete. Part I: Developments, Principles, Raw Materials." *Case Studies in Construction Materials*, no. 17, e01290. <https://doi.org/10.1016/j.cscm.2022.e01290>.
3. Baby, F., B. Graybeal, P. Marchand, and F. Toutlemonde. 2013. "UHPFRC Tensile Behavior Characterization: Inverse Analysis of Four-Point Bending Test Results." *Materials and Structures* 46 (8): 1337–1354. <https://doi.org/10.1617/s11527-012-9977-0>.
4. CPCI (Canadian Precast/Prestressed Concrete Institute). 2017. *CPCI Design Manual: Precast and Prestressed Concrete*. 5th ed. Ottawa, ON, Canada: CPCI.
5. El-Helou, R. G., Z. B. Haber, and B. A. Graybeal. 2022. "Mechanical Behavior and Design Properties of Ultra-High-Performance Concrete." *ACI Materials Journal* 119 (1): 181–194. <https://doi.org/10.14359/51734194>.
6. Yoo, D.-Y., and Y.-S. Yoon. 2016. "A Review on Structural Behavior, Design, and Application of Ultra-High-Performance Fiber-Reinforced Concrete." *International Journal of Concrete Structures and Materials* 10 (2): 125–142. <https://doi.org/10.1007/s40069-016-0143-x>.
7. Sylaj, V., A. Fam, M. Hachborn, and R. Burak. 2020. "Flexural Response of Double-Wythe Insulated Ultra-High-Performance Concrete Panels with Low to Moderate Composite Action." *PCI Journal* 65 (1): 24–40. <https://doi.org/10.15554/pcij65.1-01>.
8. Sylaj, V., and A. Fam. 2021. "UHPC Sandwich Panels with GFRP Shear Connectors Tested under Combined Bending and Axial Loads." *Engineering Structures*, no. 248, 113287. <https://doi.org/10.1016/j.engstruct.2021.113287>.
9. Einea, A., D. C. Salmon, G. J. Fogarasi, T. D. Culp, and M. K. Tadros. 1991. "State-of-the-Art of Precast Concrete Sandwich Panels." *PCI Journal* 36 (6): 78–98. <https://doi.org/10.15554/pcij.11011991.78.98>.
10. Peng, C., Y. J. Kim, and J. Zhang. 2021. "Thermal and Energy Characteristics of Composite Structural Insulated Panels Consisting of Glass Fiber Reinforced Polymer and Cementitious Materials." *Journal of Building Engineering*, no. 43, 102483. <https://doi.org/10.1016/j.job.2021.102483>.
11. PCI Precast Sandwich Wall Panels Committee. 2011. *State of the Art of Precast/Prestressed Concrete Sandwich Wall Panels*. 2nd ed. *PCI Journal* 56 (2): 131–176.
12. ACI (American Concrete Institute). 2019. Building Code Requirements for Structural Concrete. ACI 318-19. Farmington Hills, MI: ACI.
13. Canadian Standards Association Group. 2019. *Design of Concrete Structures*. CSA A23.3-19. Toronto, ON, Canada: CSA Group.
14. Fuchs, W., R. Eligehausen, and J. E. Breen. 1995. "Concrete Capacity Design (CCD) Approach for Fastening to Concrete." *ACI Structural Journal* 92 (1): 73–94. <https://doi.org/10.14359/1533>.
15. Grosser, P., J. Silva, R. Eligehausen, and D. Meinheit. 2022. "Concrete Breakout Strength of Anchors under Shear Loading." *ACI Structural Journal* 119 (6): 259–273. <https://doi.org/10.14359/51734806>.
16. Tarawneh, A. N., B. E. Ross, and T. E. Cousins. 2020. "Shear Behavior and Design of Post-installed Anchors in Thin Concrete Members." *ACI Structural Journal* 117 (3): 311–322. <https://doi.org/10.14359/51723508>.
17. Prejs, A., A. Jawdhari, and A. Fam. 2023. "Shear Strength of Post-installed Connectors in Thin UHPC Precast Walls." *Structures*, no. 48, 492–510. <https://doi.org/10.1016/j.istruc.2022.12.102>.
18. Choi, S., C. Joh, and S.-C. Chun. 2015. "Behavior and Strengths of Single Cast-in Anchors in Ultra-high-perfor-

mance Fiber-reinforced Concrete (UHPFRC) Subjected to a Monotonic Tension or Shear.” *KSCE Journal of Civil Engineering* 19 (4): 964–973. <https://doi.org/10.1007/s12205-013-0246-8>.

19. Dingqiang, F., R. Yu, L. Kangning, T. Junhui, S. Zhonghe, W. Chunfeng, W. Shuo, G. Zhenfeng, H. Zhengdong, and S. Qiqi. 2021. “Optimized Design of Steel Fibres Reinforced Ultra-high performance Concrete (UHPC) Composites: Towards to Dense Structure and Efficient Fibre Application.” *Construction and Building Materials*, no. 273, 121698. <https://doi.org/10.1016/j.conbuildmat.2020.121698>.
20. ASTM Subcommittee E06.13. 2018. *Standard Test Methods for Strength of Anchors in Concrete Elements*. ASTM E488/E488M-18. West Conshohocken, PA: ASTM International.

Notation

c	= edge distance to the free edge
d_c	= connector diameter
d_o	= outer diameter of connector
f'_c	= concrete compressive strength
l	= embedment (bearing) length
l_s	= support span length
t	= panel thickness
V	= shear loading
V_u	= concrete breakout shear capacity
ρ	= fiber content
ρ_f	= fiber content by volume

About the authors



Hoda Osman is a PhD student in the Department of Civil Engineering at Queens University in Kingston, ON, Canada.



Amir Fam is the Canada Research Chair (Tier I) Professor in Climate Change Resilient Infrastructure at Queens University.

Abstract

The replacement of normal-strength concrete in precast concrete panels with ultra-high-performance concrete (UHPC) results in a significant reduction in panel thickness. This poses a challenge when connecting these very thin wall or floor panels to the frame of the building, for example, because of the small embedment of the connectors. This paper examines the behavior of cast-in-place connectors in ultra-thin UHPC panels under direct shear loading for a variety of connector types, including two threaded bolts (carriage bolt and L-shaped bolt) and two female headed inserts (zamac insert and flower-shaped insert). The connections were tested under shear loading in 104 panel tests with varying parameters for panel thickness, connector diameter, polyoxymethylene (POM) fiber content, support span length, and edge distance of the connector. The failure mode observed by most connector types was consistently a V-shaped concrete cone breakout. Cast-in connectors outperformed the postinstalled connectors by 110%. Connectors embedded in 38 mm (1.5 in.) thick panels showed up to a 120% increase in strength compared with 15 mm (0.6 in.) thick panels. In addition, a 45% to 65% increase in strength occurred when the cast-in-place connection was embedded at a 64 mm (2.5 in.) edge distance compared with a 25 mm (1 in.) distance. Existing shear strength equations for normal-strength concrete grossly overestimated connector strength. A design equation is proposed for cast-in connectors in thin UHPC panels with POM fibers by introducing a strength amplification factor to an existing equation for postinstalled connectors.

Keywords

Bolt, cast-in, connector, fiber, polyoxymethylene, POM, postinstalled, shear, UHPC, ultra-high-performance concrete, zamac insert.

Review policy

This paper was reviewed in accordance with the Precast/Prestressed Concrete Institute's peer-review process. The Precast/Prestressed Concrete Institute is not responsible for statements made by authors of papers in *PCI Journal*. No payment is offered.

Publishing details

This paper appears in *PCI Journal* (ISSN 0887-9672) V. 71, No. 1, January–February 2026, and can be found at <https://doi.org/10.15554/pci.71.1-01>. *PCI Journal* is published bimonthly by the Precast/Prestressed Concrete Institute, 8770 W. Bryn Mawr Ave., Suite 1150, Chicago, IL 60631. Copyright © 2026, Precast/Prestressed Concrete Institute.

Reader comments

Please address any reader comments to *PCI Journal* editor-in-chief Tom Klemens at tklemens@pci.org or Precast/Prestressed Concrete Institute, c/o *PCI Journal*, 8770 W. Bryn Mawr Ave., Suite 1150, Chicago, IL 60631. [f](#)